



Key technology for the construction and inspection of long-distance underwater tunnel for 1000 kV gas-insulated transmission line

Xiao-Ping Zhang^{1,2} · Shao-Hui Tang^{1,2} · Quan-Sheng Liu^{1,2} · Hao-Jie Wang^{1,2} · Xin-Fang Li^{1,2} · Peng Chen³ · Hao Liu⁴

Received: 12 November 2021 / Accepted: 22 October 2022 / Published online: 14 December 2022
© Springer-Verlag GmbH Germany, part of Springer Nature 2022

Abstract

With the rapid development of urbanization and industrialization, electric power consumption continues to increase on a worldwide basis. Traditional overhead transmission lines cannot satisfy the requirements for modernization of power distribution systems. Cable tunnels with ultra-high-voltage and complex network have become the trend of urban power transmission lines for their advantages in flexibility, expandability, and convenient maintenance. Although cable tunnels have good adaptability in power transmission, their application is severely restricted by construction and inspection technologies. Especially for long-distance cross-river tunnels installed with 1000 kV equipment, there is still a lack of reliable solutions to deal with complex challenges encountered during the construction and inspection of ultra-high-voltage cable tunnels. In the present study, complexity features of the first underwater gas-insulated transmission line for 1000 kV power in the world, Sutong GIL Yangtze River Crossing Cable Tunnel, have been analyzed. Engineering challenges encountered during the construction and inspection of long-distance cable tunnel have been discussed. Key technologies including embankment deformation control, gas explosion prevention, synchronous transportation organization, dust-free equipment installation, and robot intelligent inspection have been developed. The application of these technologies has enabled the safe and efficient construction and inspection of a high-quality cross-river cable tunnel.

Keywords Cable tunnel · Shield TBM · Engineering feature · Construction challenge · Key technology

Introduction

Since Thames tunnel was constructed between 1825 and 1843 (Tobriner 1984; Muir Wood 1994), shield tunnels have achieved great success in traditional industries. Data from 2005 to 2010 indicates that the number of shield tunnels with diameters from less than 3.0 m to over 15.0 m is up to 350 units (Home 2010; Alavi Gharahbagh et al. 2013; Jakobsen

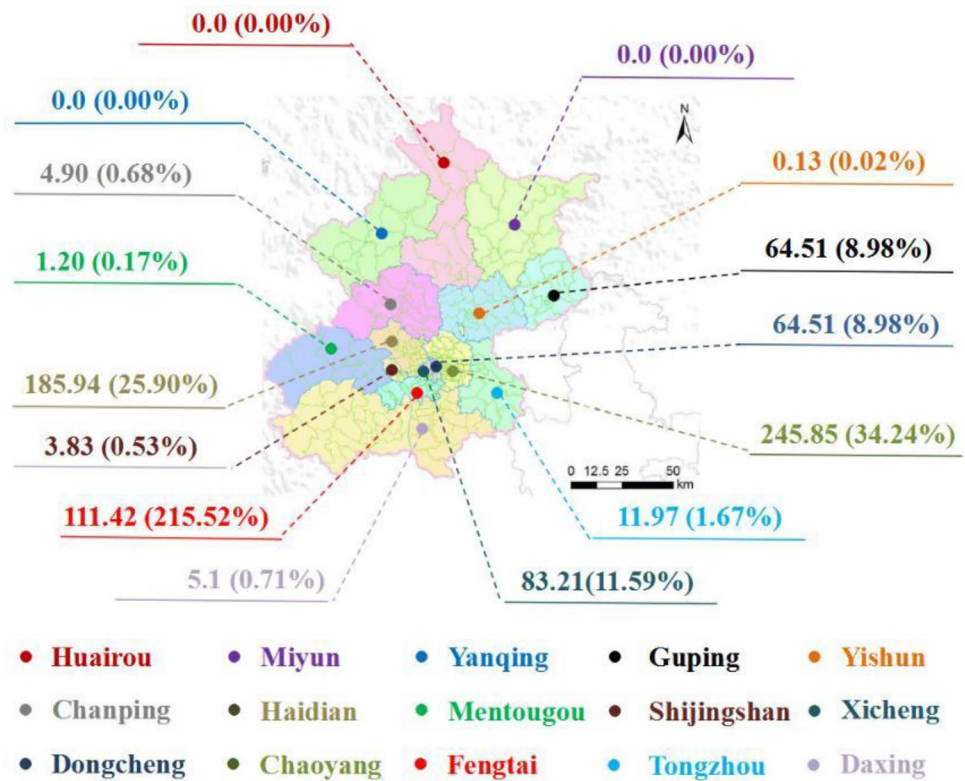
and Lohne 2013; Zhang et al. 2021). Most of them are subway tunnels, highway tunnels, railway tunnels, pedestrian tunnels, and water tunnels (Abdullah 2016; Kaliampakos et al. 2016; Li et al. 2017, 2018; Li and Ingason 2018; Hong et al. 2021; Tang et al. 2021a). Especially for subway tunnels, an unprecedented construction boom has occurred for the expanding demands of urban transportation network (Jin et al. 2018; Wang et al. 2018; Zhang et al. 2018a; Tang et al. 2022).

With the development of urbanization and industrialization, shield tunnels have been expanding rapidly in emerging industries such as power transmission, telecommunication service, central heating, and other public service (Wang et al. 2007; Masuda et al. 2008; Canto-Perello et al. 2016; Delmastro et al. 2016a, b; Vähäaho 2016; Jiménez et al. 2018; Wang et al. 2018; Zhao et al. 2018). Taking power transmission as an example, traditional overhead transmission lines have been difficult to satisfy the requirements for the modernization of power distribution system (Wang et al. 2007; Fang et al. 2014; He 2016). Cable tunnels with high-voltage and complex network

✉ Xiao-Ping Zhang
jxhkzhang@163.com

¹ Key Laboratory of Safety for Geotechnical and Structural Engineering of Hubei Province, School of Civil Engineering, Wuhan University, Wuhan 430072, China
² State Key Laboratory of Water Resources and Hydropower Engineering Science, Wuhan University, Wuhan 430072, China
³ China Railway 14th Bureau Group Shield Engineering Co., Ltd., 211800 Nanjing, China
⁴ China Railway Siyuan Survey and Design Group Co., Ltd., Wuhan 430063, China

Fig. 1 The distribution of cable tunnels in 15 administrative districts of Beijing, China, as of January 2015 (Wang et al. 2016a; Zhao et al. 2017)



have become the trend of urban power transmission lines for their advantages in flexibility, expandability, and convenient maintenance (Wang et al. 2007; Yang and Peng 2016). Take Beijing, China, as an example, cable tunnels have reached 718 km at the beginning of 2015 (Wang et al. 2016a; Zhao et al. 2017). They are unevenly distributed in 15 administrative districts (Fig. 1). Details have been shown in Table 1.

Although cable tunnels are expanding rapidly, there are still complex and uncertain constraints (Goel et al. 1995; Wang et al. 2007). Especially for long-distance ultra-high-voltage cable tunnels, engineering challenges resulting from tunnel construction and equipment inspection are considered as deficiencies restricting the further development of gas-insulated transmission lines (Xie and Yang 2012; Yang et al. 2013; Hashemnejad and Hassanpour 2017; Aydan and

Table 1 Parameters of cable tunnels in Beijing, China, as of January 2015 (Wang et al. 2016a; Zhao et al. 2017)

Times	Total mileage (km)	Section type	Sectional dimension (m)	Length ratio (%)
1970~1980s	82	Rectangle	2×2.5	93.7
		Straight wall arch	2×2.3	0.4
		Round	Φ2.15	5.9
1990s	300	Rectangle	2.6×2.9	75.7
		Straight wall arch	2×2.3	0.5
		Round	Φ1.95	5.1
		Rectangle	2×2.35	18.7
2000~2015	336	Rectangle, parallel straight wall arch	2.6×5.3	68.7
		Straight wall arch, parallel straight wall arch and stacked double rectangle	2.6×2.9	12.4
		Rectangle	2.6×2.9/Φ2.15	2.3
		Round	Φ3	6.7
		Rectangle	2.6×2.4	9.9

Hasanpour 2019; Bilgin and Acun 2021; Tang et al. 2021a). These problems have attracted broad attention from tunnel contractors, TBM manufacturers, and consultants.

A preliminary literature survey indicates that a series of technologies have been proposed to deal with construction and inspection challenges in simple working conditions (Goel et al. 1995; Wang et al. 2007; Neumann et al. 2010; Yang 2016). For instance, Kasper and Meschke (2006), Min et al. (2015), Zhang et al. (2017, 2018b), and Ding et al. (2019) optimized slurry pressure, grouting pressure, and grouting volume according to ground deformation characteristics. The optimization parameters are suitable for specific geological conditions and cannot be directly applied in dense sandy ground at Sutong GIL Yangtze River Crossing Cable Tunnel. Lin et al. (2013), Gui and Chen (2013), Fang et al. (2014), Bouayad and Emeriault (2017), Jin et al. (2018), Moghaddasi and Noorian-Bidgoli (2018), and Yao et al. (2020) studied the relationship between ground deformation, tunneling parameters and geological parameters. The relationship obtained by numerical simulation or data fitting is limited in adaptability and accuracy. Jia et al. (2012), Yu et al. (2012), Guo et al. (2013a, b), Feng et al. (2016), and Chen et al. (2018) proposed several trackless transportation models to accelerate the material transportation progress of short and medium distance tunnels. They are difficult to satisfy the material transportation requirements of long-distance single-headed cable tunnels with complex internal structure. Benato and Paolucci (2010), Neumann et al. (2010), Poehler and Rudenko (2012), Tenzer et al. (2016), and Magier et al. (2017) introduced the feature and criteria in the automated assembly and laying process for faster installation of the directly buried gas-insulated line (GIL). The feature and criteria cannot be applied to dust-free installation of dual-circuit 1000 kV GIL equipment in cable tunnel. Victores et al. (2011), Xu et al. (2013), Montero et al. (2015), Seet et al. (2018), Agnisarman et al. (2019), and Dai et al. (2020) summarized the defects of manual inspection procedure in high cost, long duration and critical risk, and generalized the advantages of visual inspection technologies in automated operation, high efficiency, and good security. However, the visual inspection technologies for traffic tunnels cannot detect the operating parameters and working environment of 1000 kV GIL equipment. In summary, there is still a lack of effective technologies to deal with construction and inspection challenges of long-distance single-headed cable tunnel equipped with 1000 kV GIL equipment.

The present study provides an overview of the first underwater gas-insulated transmission line for 1000 kV power in the world, Sutong GIL Yangtze River Crossing Cable Tunnel. Complexity features and engineering challenges encountered during the construction and inspection of cross-river cable tunnel are analyzed. Key technologies

including embankment deformation control, gas explosion prevention, synchronous transportation organization, dust-free equipment installation, and robot intelligent inspection have been developed. The application of these technologies is not only beneficial to Sutong GIL Yangtze River Crossing Cable Tunnel, but also to similar long-distance cross-river cable tunnels in the future.

Background

Project overview

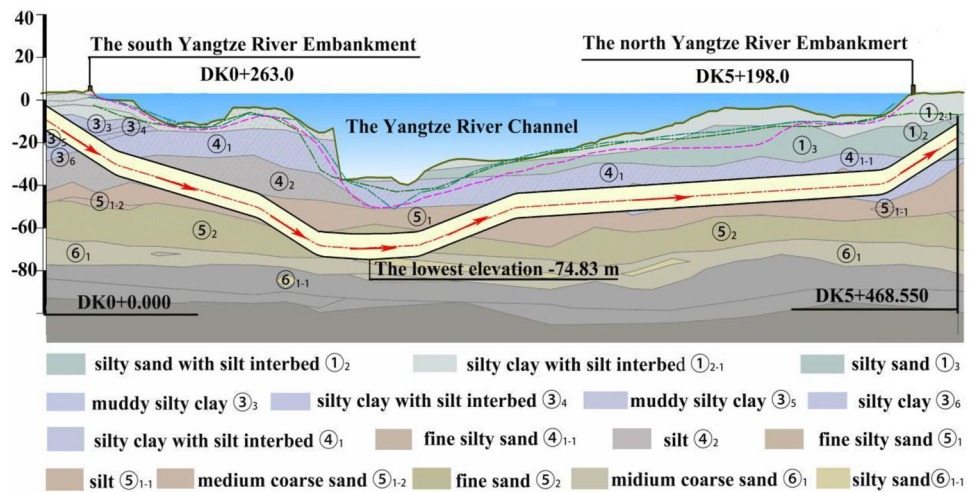
In order to promote energy structure transformation and sustainable economic development of the Yangtze River Delta, State Grid Corporation of China has decided to construct the Huainan ~ Nanjing ~ Shanghai 1000 kV ultra-high-vacuum (UHV) power transmission line, which will cooperate with the Huainan ~ Zhejiang ~ Shanghai 1000 kV UHV power transmission line to form a UHV ring network to improve the capacity of East China Load Center in receiving UHV power from other areas.

Sutong GIL Yangtze River Crossing Cable Tunnel is a key project, which controls the construction progress of Huainan ~ Nanjing ~ Shanghai 1000 kV UHV power transmission line. It is designed for UHV cables to cross the Yangtze River. The overall length from the launching shaft in Suzhou to the receiving shaft in Nantong is about 5468 m (Fig. 2). The excavation diameter of slurry shield TBM is 12.07 m. The line shape is extremely complicated, with a maximum longitudinal slope of 5% and a minimum curve radius of 2000 m. The tunnel underpassing the Yangtze River channel with the lowest elevation of -74.80 m and the maximum water and soil pressure of 0.95 MPa. It is one of the deepest buried soft ground tunnels with the highest water and soil pressure in China.

Geology and soil properties

Sutong GIL Yangtze River Crossing Cable Tunnel is located at the front edge of the alluvial plain of the Yangtze River Delta, where the engineering geology is complex due to the intricate sedimentary facies. According to the geotechnical baseline reports (GBRs) and geotechnical data reports (GDRs), the sedimentary sequences of the incised-valley is relatively complete with five sedimentary facies: the fluvial channel, floodplain, estuary, shallow marine, and delta. Figure 2 illustrates the distribution of soil layers along the tunnel alignment. Statistics on soil content indicate that the tunnel is 54% in abrasive sand and 46% in silt and clay.

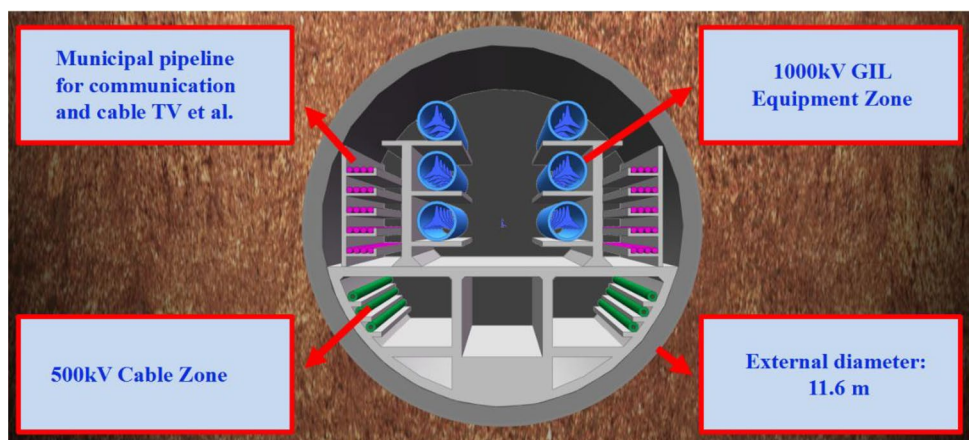
Fig. 2 Geologic profile of Sutong GIL Yangtze River Crossing Cable Tunnel (Tang et al. 2020, 2021a, b)



The internal structure of UHV cable tunnel

Compared with traditional highway tunnels and railway tunnels, Sutong GIL Yangtze River Crossing Cable Tunnel is more complex in internal structure. As shown in Fig. 3, the outer diameter and inner diameter of final lining consisting of 8 concrete segments (including 7 standard segments and 1 key segment) are 11.6 m and 10.5 m. The interior space of segment ring can be divided into two parts by the roof of box culvert. The upper part is applied for the installation of 1000 kV GIL equipment and municipal pipelines, while the lower part is utilized for the arrangement of 500 kV cable and inspection gallery. In order to circulate the air in the long-distance single-headed tunnel, two flexible ducts with a diameter of $D = 1.50$ m are installed on the top of final lining. As dirty and harmful gas is pumped out in time, the safety of workers and equipment can be maximized.

Fig. 3 Schematic diagram of the completed cable tunnel

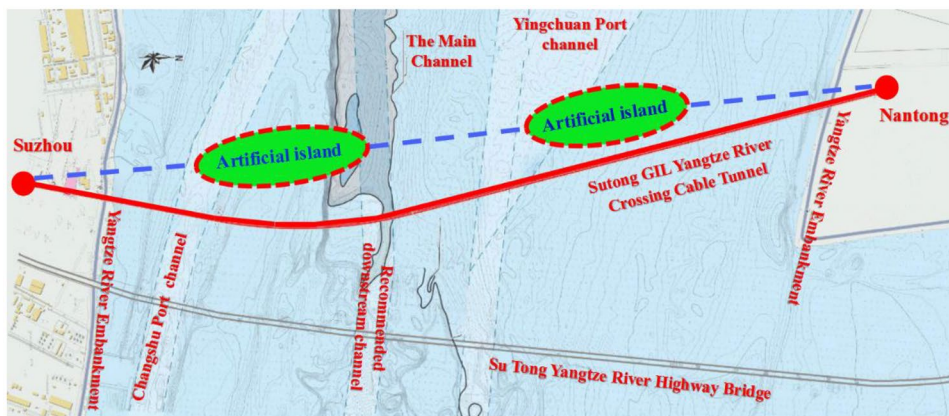


Feasibility study of the long-distance cross-river cable tunnel

As shown in Fig. 4, there are two construction schemes available for the gas-insulated power transmission line crossing the Yangtze River. The first scheme is traditional overhead transmission line. Feasibility studies indicate that two towers with a height of more than 400 m are required for the high-voltage power transmission. The area of artificial islands utilized for tower bases is expected to exceed 22,680 m². The large artificial islands not only interfere with river transport but also destroy ecological environment. Moreover, preliminary estimation shows that more than 400,000 m³ of concrete needs to be transported to the artificial islands in the Yangtze River for tower foundation construction. It is high labor and money cost.

The second scheme involves the construction of a long-distance cross-river cable tunnel. The total length

Fig. 4 Construction schemes for the gas-insulated transmission line crossing the Yangtze River



and excavation diameter are 5468 m and 12.07 m respectively. Variable longitudinal slope with a maximum value of 5% is designed to accommodate the valley landscape of river bottom. The curvature with a minimum radius of 2000 m is designed to keep away from the severe eroded area of Yangtze River channel. Compare with the overhead transmission line, the cable tunnel has significant advantages not only in power transmission (such as flexibility, expandability, and maintenance), but also in environmental protection (such as waterway maintenance, port planning, and flood control). It has been approved by project owners for gas-insulated transmission line to cross the Yangtze River.

Engineering feature and construction challenge

Ground deformation and surface crack of Yangtze River embankment

As shown in Fig. 5, slurry shield TBM underpassing the south Yangtze River embankment at the location of DK0+263. The overburden layers are muddy silty clay and silty clay (Table 2). Tunneling in such a susceptible overburden ground is difficult to control deformation. Excessive slurry pressure, grouting pressure, and grouting volume result in ground uplift, while insufficient slurry pressure,

Fig. 5 The overburden layers of south Yangtze River embankment

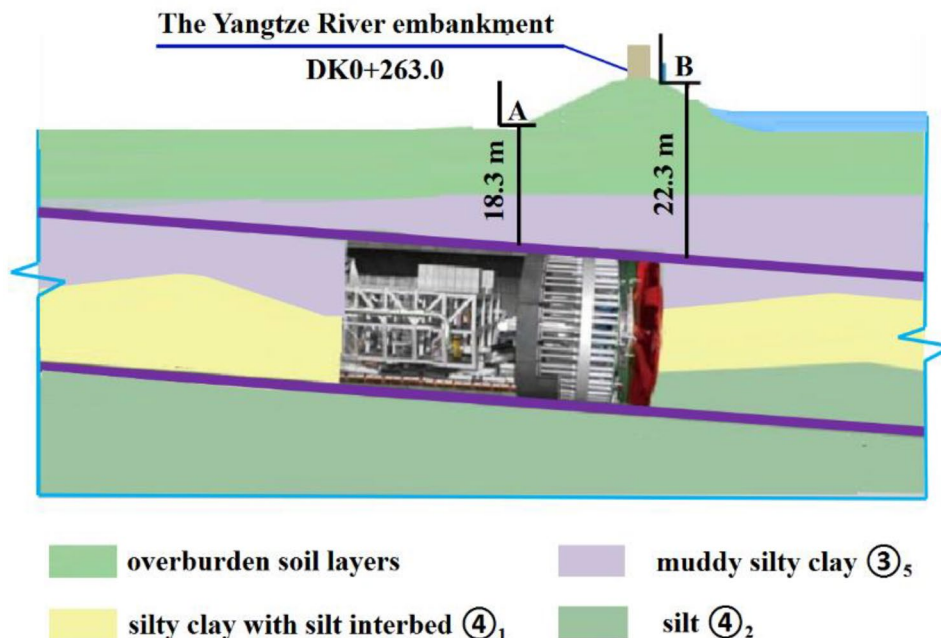


Table 2 The overburden soil parameters of south Yangtze River embankment

Soil types	Cohesion c (kPa)	Internal friction angle φ ($^{\circ}$)	Moisture content ω (%)	Porosity n	Density ρ (g/cm ³)
Muddy silty clay @ ₅	10.63	21.17	57.65	0.52	1.79
Silty clay with silt interbed @ ₁	7.30	23.10	49.66	0.50	1.81
Silt @ ₂	4.00	27.23	39.18	0.46	1.87

grouting pressure, and grouting volume lead to ground collapse. As a critical structure to prevent floods, the deformation control and crack prevention of Yangtze River embankment by controlling slurry pressure, optimizing synchronous grouting, and strengthening deformation monitoring should be considered carefully before tunneling.

Methane leakage and gas explosion in biogenetic gas ground

According to geotechnical baseline reports (GBRs) and geotechnical data reports (GDRs), there is biogenetic gas in silty clay, silt, and fine silty sand in the excavation interval of DK0+0~DK1+780. It is distributed in the form of lentils, clumps, and sacs. Static penetration tests indicate that the shut-in pressure of biogenetic gas is 0.25~0.30 MPa. The average capacity of each gas storage point is about 5.0 m³. Composition tests indicate that it is composed of methane (86.74%), nitrogen (9.73%), oxygen (2.79%), carbon dioxide (0.64%), argon (0.09%), and ethane (0.01%). Shield tunnel construction in gas-rich ground is dangerous. Once the leakage occurs, biogenetic gas will penetrate into the tunnel from pressure cabin and shield tail. Security emergencies such as explosion and suffocation are prone to occur. However, mechanism studies and prevention technologies for gas explosion focus on mining industry; their application in tunnel projects is still in infancy. To the best of our knowledge, there is still a lack of comprehensive explosion-proof technologies for biogenetic gas ground tunneling using slurry shield TBM.

Trackless transportation congestion in long-distance tunnel

Construction and building materials (including concrete segment, precast box culvert, concrete, cement mortar, slurry pipe, water pipe, and other auxiliary materials) are transported from the ground to the working face by trackless vehicles. As shown in Fig. 6, the road for material transportation in the tunnel can be divided into two sections. Since side box culvert has been poured with concrete, the first section near tunnel portal consists of three traffic lanes. When the vehicle travels to the second section where side box culvert has not been poured with concrete (or the concrete has not hardened), only one traffic lane can be provided for trackless transportation. If one vehicle encounters another coming in the opposite direction, traffic congestion will be prone to occur. Especially when the single traffic lane is too long (the construction progress of side culvert lags behind tunnel excavation), it will be a prominent factor restricting tunnel construction efficiency (Feng et al. 2016; Chen et al. 2018).

Dust-free environment for GIL equipment installation

Compared with traditional traffic tunnel, utility tunnel, and water tunnel, the installation of 1000 kV ultra-high vacuum GIL equipment (Fig. 7) puts forward higher requirements for tunnel internal environment. The air cleanliness should satisfy ISO Class 9 (ISO E. 14644-1 1999). Air humidity should be lower than 80%, and illuminance should be higher than 75

Fig. 6 The distribution of traffic lane in the cable tunnel (Chen et al. 2018; Liang et al. 2018)

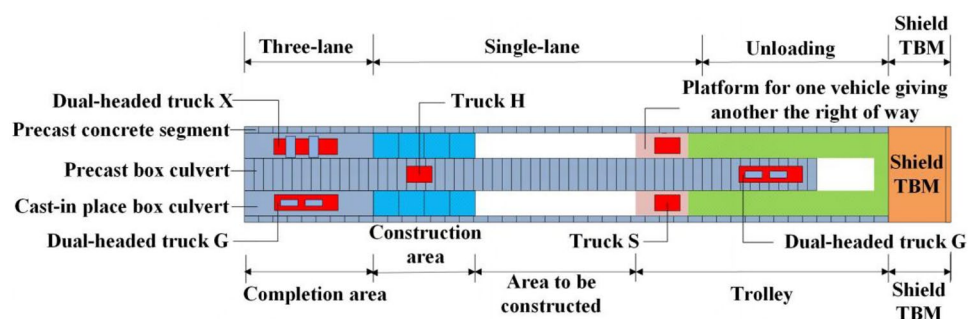
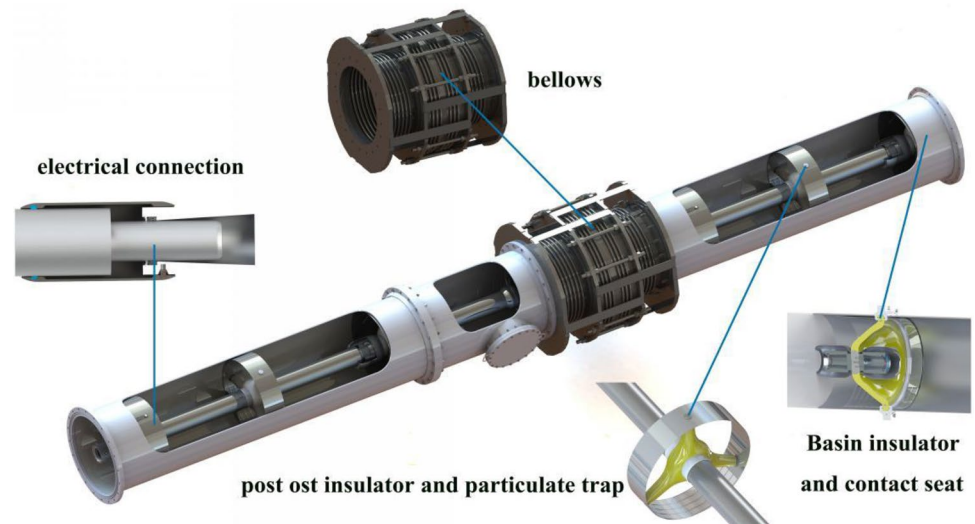


Fig. 7 The 1000 kV ultra-high-vacuum GIL equipment



Lx (DL/T 5838–2021 2021). When traditional methods are utilized for GIL equipment installation, it is difficult for tunnel internal environment to satisfy such high requirements. Special environmental control equipment needs to be designed and arranged in the limited tunnel interior space to ensure the successful installation of GIL equipment.

Unfavorable manual inspection for UHV cable tunnel

As shown in Fig. 2, the overall length of Sutong GIL Yangtze River Crossing Cable Tunnel is up to 5468 m. If manual inspection is utilized for the long-distance cable tunnel, it will be a time-consuming, laborious, and inefficient work. Moreover, the complex internal structure brings great challenge for manual inspection. The staggered cable equipment obstructs the sight of workers. Equipment failures and safety hazards are prone to be ignored. Last but not least, the voltage level of gas-insulated transmission lines is up to 1000 kV. Electric shock accidents are prone to occur during manual inspection. As a result, a safe and efficient inspection method is required for the ultra-high-vacuum cable tunnel.

Key technology for safe and efficient construction

The objective of this section is to introduce key technologies for safe and efficient construction and inspection of Sutong GIL Yangtze River Crossing Cable Tunnel. Details on the embankment deformation control, gas explosion prevention, synchronous transportation organization, dust-free equipment installation, and robot intelligent inspection will be set out in the following sections.

Control on the deformation of Yangtze River embankment

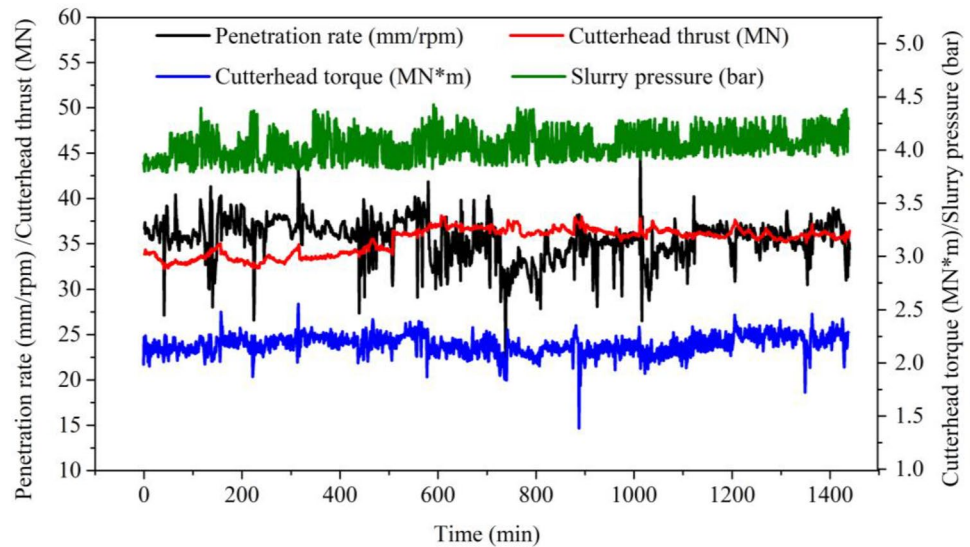
Slurry pressure

According to the formulas recommended by Min et al. (2015), the active (or static) earth pressure at the center of cutterhead at the locations A and B (Fig. 5) can be calculated as 0.088 MPa (or 0.123 MPa) and 0.101 MPa (or 0.142 MPa). With the addition of groundwater pressure ($P_{wA} = 0.226$ MPa and $P_{wB} = 0.266$ MPa) and the pressure difference ($\Delta P = 0.030$ MPa), slurry pressure at the locations A and B will be up to 0.344~0.379 MPa and 0.397~0.438 MPa respectively. Since slightly higher face support pressure reduces ground loss (Lin et al. 2013), the recommended slurry pressure for shield TBM underpassing the south Yangtze River embankment is 0.379~0.438 MPa. Details on the slurry pressure and excavation parameters have been illustrated in Fig. 8.

Synchronous grouting

The cement mortar utilized for synchronous grouting is made by mixing Portland cement (P·O 42.5), flyash, bentonite, river sand, and admixture with appropriate water. Compared with regular excavation interval, the grouting materials applied for slurry shield TBM underpassing the Yangtze River embankment are much higher in cement content (Table 3). Experimental studies indicate that when the cement content increases from 2.4 to 8.4%, the initial setting time decreases from 12 to 8 h, and the consolidated strength after 1 day increases from 0.32 MPa to 0.86 MPa. The cement mortar with shorter initial setting

Fig. 8 The slurry pressure and excavation parameters for shield TBM underpassing the south Yangtze River embankment



time and higher early consolidated strength reduces the deformation of susceptible overburden ground.

The grouting pressure should theoretically be equal to the overburden pressure (Wang et al. 2016b). The overburden pressure (the sum of static earth pressure and water pressure) at the locations A and B (Fig. 5) is 0.349 MPa and 0.408 MPa. Considering pressure loss in the grouting pipeline, the compensatory pressure of 0.05 MPa should be added with reference to the Nanjing Yangtze River Tunnel in similar conditions (Guo and Dai 2013). As a result, the grouting pressure of 0.399~0.458 MPa is recommended for shield TBM underpassing the Yangtze River embankment. As for the grouting volume, case studies of shield TBMs tunneling in similar ground indicate that the filling ratio of cement mortar is $\alpha = 130 \sim 150\%$ (Guo and Dai 2013). It is recommended as the filling ratio of cement mortar in this project. According to the formulas recommended by Lin et al. (2013), the grouting volume at one circle of excavation should be $V = 22.07 \sim 26.20 \text{ m}^3/\text{ring}$.

Deformation monitoring

In order to control the deformation of the Yangtze River embankment, comprehensive monitoring schemes were performed with instrumentation points along the tunnel alignment. As shown in Fig. 9a, four rows of monitoring

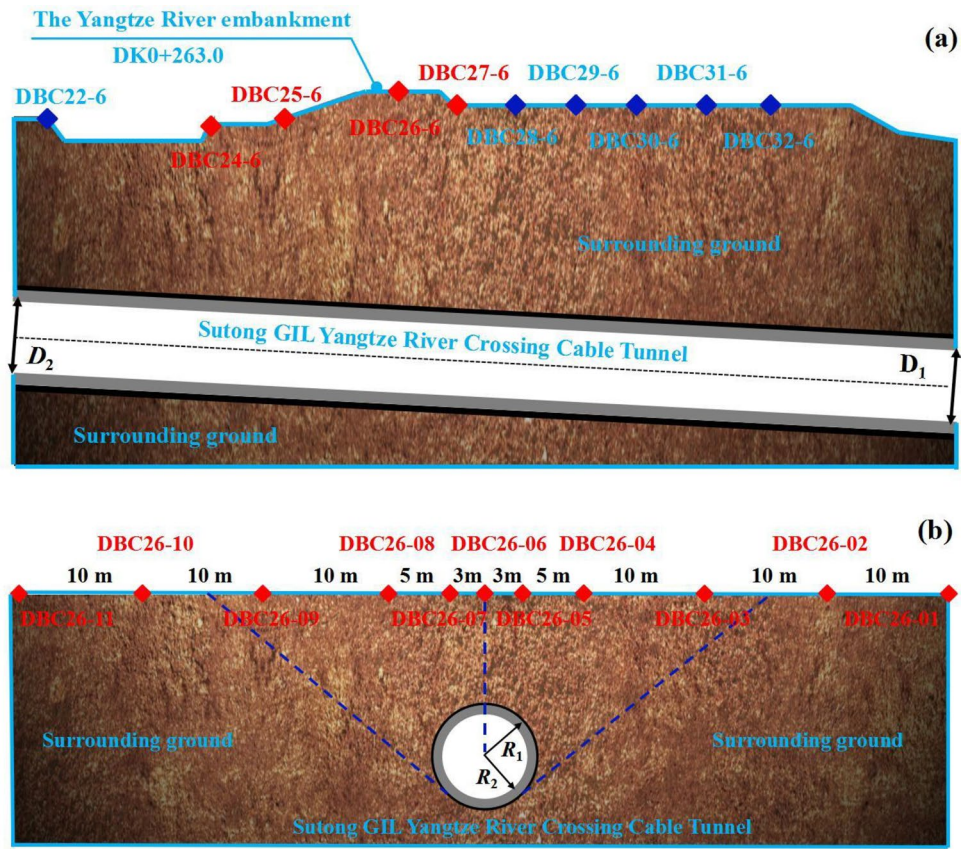
points numbered from DBC24 to DBC27 were arranged at the embankment. For each row, at least 9 monitoring points, in the direction perpendicular to the tunnel alignment and at 3 m, 5 m, and 10 m intervals (Fig. 9b) were surveyed by precise leveling techniques. Once excessive surface deformation was monitored, reinforcement technologies such as cement grouting and sleeve valve pipe grouting would be applied to prevent ground fissure expansion.

Slurry shield TBM underpassing the Yangtze River embankment on August 12, 2017. The ground surface deformation was monitored from August 09, 2017 to August 18, 2017. Taking the row numbered DBC26 as an example, the ground surface deformation was plotted against the monitoring date (Fig. 10). The results indicated that ground surface bulged during slurry shield TBM underpassing the monitoring section. The maximum deformation occurred on August 12, 2017 was 18.53 mm. Since it was less than the limited deformation (30 mm), micro-cracks caused by soil disturbance were considered not to damage the embankment structure. Grouting reinforcement for the Yangtze River embankment was considered unnecessary. In order to determine whether the ground deformation had been stable, the embankment was monitored again between June 3, 2018 and June 11, 2018. The results indicated that the ground deformation had been stabilized between -3.99 and 0.33 mm, with an average value of -2.08 mm.

Table 3 The mix proportion of cement mortar used to backfill the gap between segment and ground

Interval	Cement (kg)	Flyash (kg)	Bentonite (kg)	Sand (kg)	Admixture (kg)	Water (kg)
Yangtze River embankment	153	171	56	1040	11.40	390
Regular excavation interval	45	271	92	1012	12.24	420

Fig. 9 The arrangement of monitoring points near the Yangtze River embankment: **a** monitoring points along the tunnel alignment, **b** monitoring points along the embankment



In addition, the embankment surface deformation recorded by the monitoring points in the row numbered DBC26 has been plotted against the horizontal distance from the tunnel centerline to the monitoring point (Fig. 11). The embankment transverse deformation during construction (from August 09, 2017 to August 18, 2017) can be well described by the Gaussian distribution curve (Fig. 11a), while that after construction (from June 3, 2018 to June 11, 2018) is small and random

(Fig. 11b). It is consistent with the results observed by Lin et al. (2013) at Qiantang River Tunnel.

The accurate control of slurry pressure promoted tunnel surface stability and minimized the disturbance to susceptible silty clay ground. Synchronous grouting optimization shortened the initial setting time and improved the early consolidation strength. With the application of these technologies, the maximum deformation (18.53 mm) was less than the limited

Fig. 10 The embankment surface deformation plotted against the monitoring date

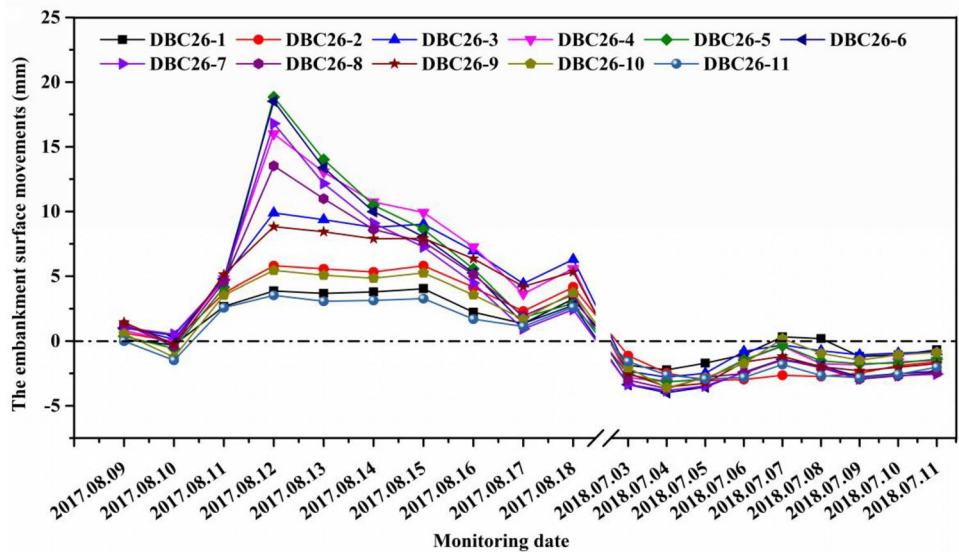
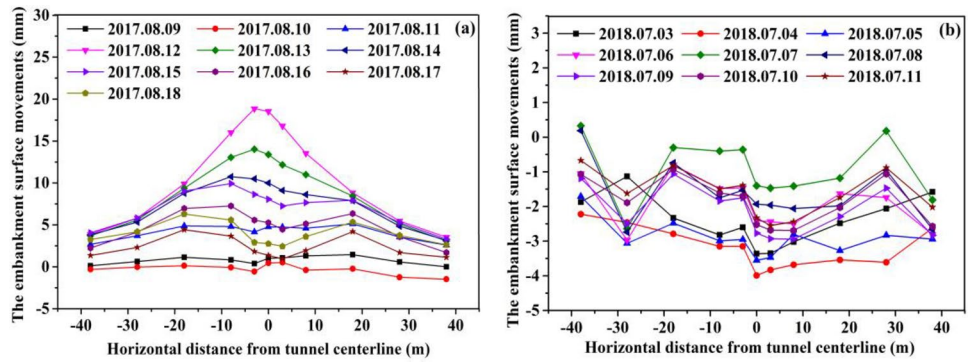


Fig. 11 The embankment surface deformation recorded by the monitoring points in the row numbered DBC26 plotted against the horizontal distance from the tunnel centerline to the monitoring point: **a** during construction, **b** after construction



deformation (30 mm). There is no penetrating ground fissure that can damage the structure of Yangtze River embankment. The deformation control technologies have protected the shield TBM underpassing the Yangtze River embankment safely.

Prevention of methane leakage in gas-rich ground

Application of clay shock method

Since the front, middle, and tail shield are 40, 60, and 80 mm smaller than the cutterhead, there will be annular gaps with thickness of 20, 30, and 40 mm between them and surrounding soil. As shown in Fig. 12, the gap 1 is filled with slurry suspension, while the gap 3 is full of cement grout. As for the gap 2, it is generally filled with slurry suspension and cement grout exuded from the front shield and the tail shield. As the diffusion rate of biogenetic gas is greater than the penetration rate of slurry suspension and cement grout,

biogenetic gas leakage will occur before the gap 2 is filled up. Moreover, engineering experience indicates that the infiltration capacity of slurry suspension and cement grout is limited. The gap 2 usually cannot be filled up. Various voids will provide access for biogenetic gas leakage.

In order to minimize biogenetic gas leakage, clay shock method has been proposed for filling the gap 2 between middle shield and surrounding soil. The clay shock is made of clay shock powder, water, and sodium silicate (Tang et al. 2021b). The preparation process has been illustrated in Fig. 13. The clay shock powder should first be mixed with appropriate water to form a suspension. The mass ratio of powder to water is 1:1.84 (Bian 2015; Du and Cheng 2017). Then, sodium silicate (40°Bé) is added into the suspension in a volume ratio of 1: 20 (Bian 2015; Tang et al. 2021b). The clay shock can be obtained only when sodium silicate is uniformly mixed with the suspension. Triaxial seepage tests have been carried out three times to determine the permeability coefficient of clay shock (confining pressure $\sigma_3 = 100$ kPa, osmotic pressure $\sigma_b = 80$ kPa, and duration time $T = 60$ days). The results indicate that the permeability coefficient of clay shock ($K_c = 3.0 \times 10^{-9}$ cm/s) is much smaller than that of the surrounding soil ($K_s = 2.75 \times 10^{-5}$ cm/s). When the gap 2 is filled up, clay shock interlayer will seal middle shield. Biogenetic gas content will be reduced under the condition that penetration path is blocked.

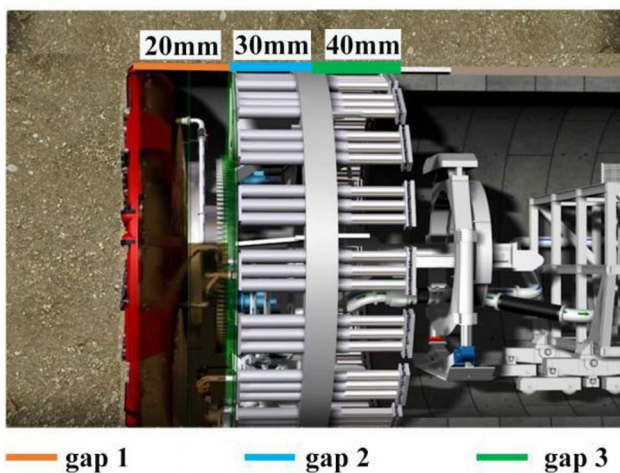
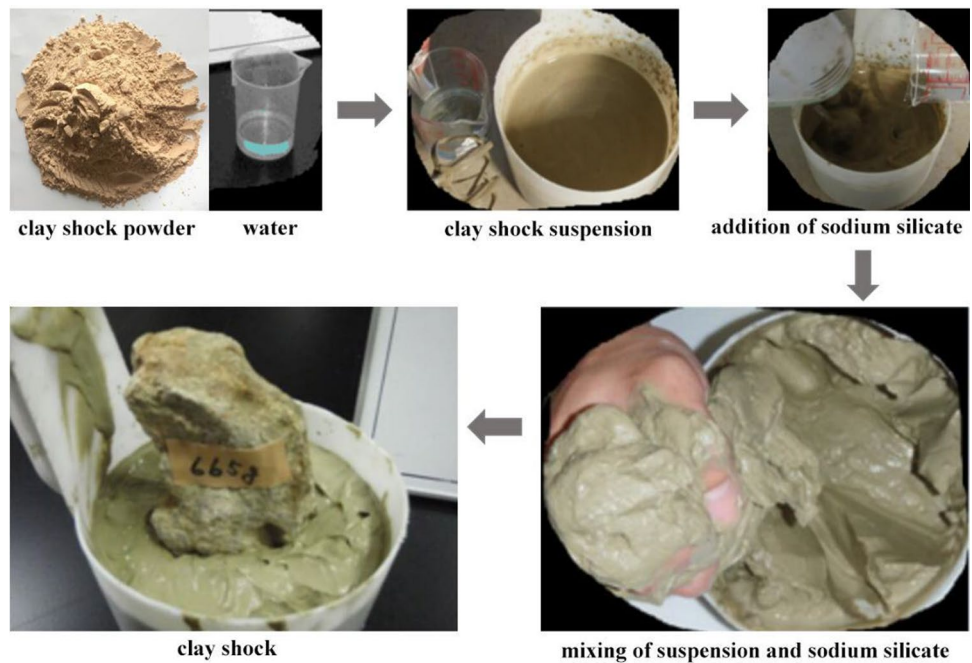


Fig. 12 Gaps between shield shell and surrounding soil. The gap 1/2/3 refers to the annular space between the front/middle/tail shield and the surrounding soil respectively

Arrangement of gas detector

There are twelve detectors arranged at slurry shield TBM to monitor gas content in real time. As shown in Fig. 14, seven of them are installed at the pressure cabin and shield body. The remaining five are installed at the trailers. Once gas content reaches 0.5%, the alarm light will be triggered and the longitudinal ventilation will be strengthened. When gas content is between 0.5 and 3.0%, the normal lighting circuit will be cut off and the emergency lighting

Fig. 13 Preparation process of clay shock: **a** preparing proper clay shock powder and water, **b** mixing clay shock powder with water, **c** adding proper sodium silicate into clay shock suspension, **d** mixing sodium silicate with clay shock suspension, **e** the completed clay shock



circuit will be turned on. With gas content increases to more than 3.0%, the high-voltage power will be cut off and the workers should be evacuated from the tunnel.

Explosion-proof of power supply equipment

Uninterruptible power supplies continuously provide energy for slurry shield TBM during tunneling. Wire and electric equipment are prone to aging under high workloads for a long time. Once power leakage occurs, the probability of gas explosion will increase dramatically. In order to minimize the risk of power leakage, uninterruptible power supplies and electrical equipment connected with them have been improved for explosion proof. As shown in Fig. 15, the input side and output side of uninterruptible power supply with four protection circuits have be electrically isolated to avoid mutual interference and ensure voltage stability. Explosion-proof power distribution device and dry-type transformer

have been used to regulate and distribute electricity. Mining cable and flameproof switch have been utilized for connecting power supply and electrical equipment. The enclosure of LED tunnel light, direction guidance system, and emergency telephone system has been explosion-proof improvement to prevent sparks during electrical equipment operation. The application of explosion-proof technologies has avoided explosion accidents from the generation, transmission, and consumption of electrical energy.

Design of gas extraction system

Gas extraction system has been designed and applied to mitigate biogenetic gas accumulation. The gas drainage pipeline with an inner diameter of $D_p = 100$ mm is arranged at the side wall of final lining. It allows a maximum mixed gas drainage capacity of $4.7 \text{ m}^3/\text{min}$. Since biogenetic gas concentration in the tunnel is 10%, the maximum biogenetic gas

Fig. 14 The arrangement of gas detectors in slurry shield TBM

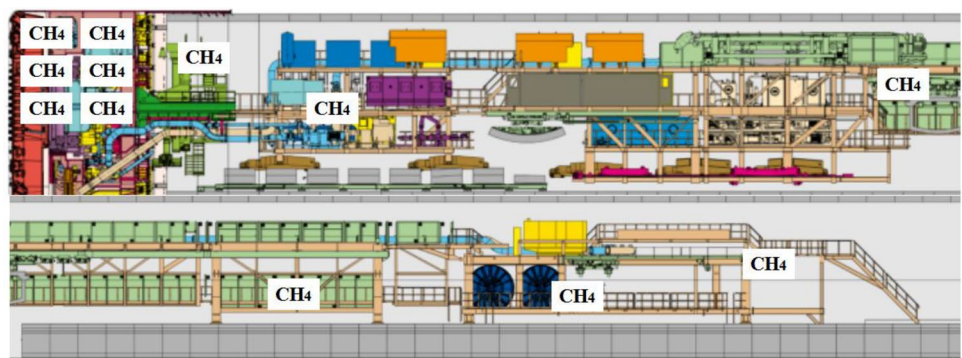
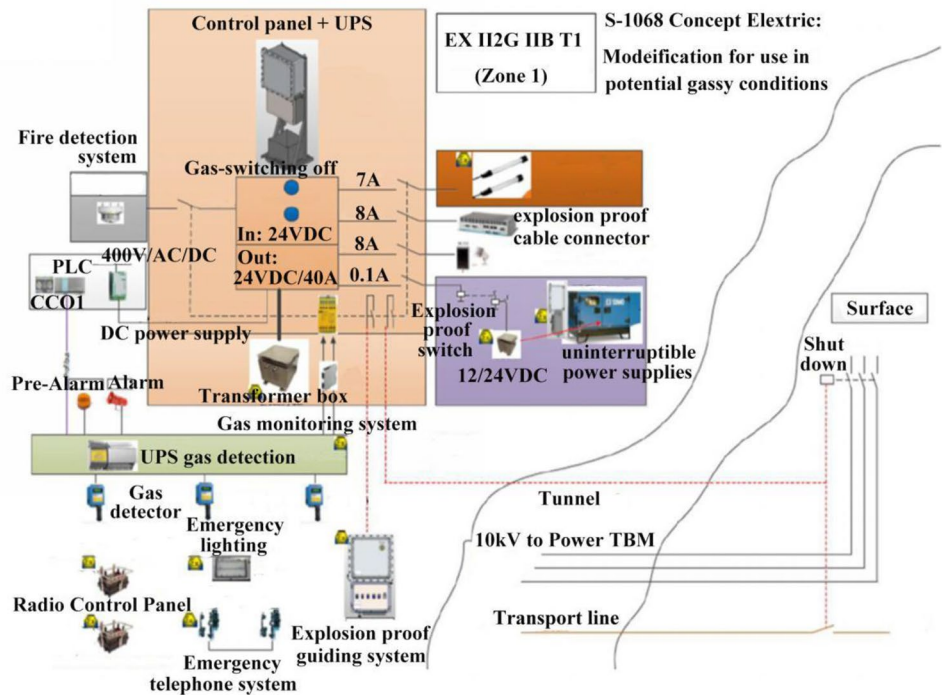


Fig. 15 Explosion proof of uninterruptible power supplies and equipment



drainage capacity should be 0.47 m³/min, which is larger than the maximum biogenetic gas spillage of 0.25 m³/min. Gas drainage pipeline is connected with the manual venting pipeline in the pressure cabin. Biogenetic gas accumulated in the pressure cabin can be discharged in time. Another end of gas drainage pipeline is connected with a ZWY20/37-G vacuum pump in the completed tunnel. The absolute pressure at the inlet and the gas flow in working condition are $P_a = 49,000$ Pa and $Q_w = 20$ m³/min respectively. In order to avoid gas accumulation due to mechanical failure, the other ZWY20/37-G vacuum pump is prepared for backup.

The application of clay shock method has prevented biogenetic gas entering the shield TBM and completed tunnel. Explosion proof of power supply equipment has minimized the probability of ignition sources such as sparks and arcs. Arrangement of gas extraction system has reduced gas content in shield TBM and completed tunnel. As shown in Fig. 16, gas detection indicates that the average content of CH₄ (0.05%) and CO (20 ppm) has been lower than the critical content of CH₄ (0.5%) and CO (24 ppm) required in Coal Mine Safety Regulations (National Mine Safety Administration of China 2004). There has been no burning or explosion accident occurred during the construction of long-distance cable tunnel.

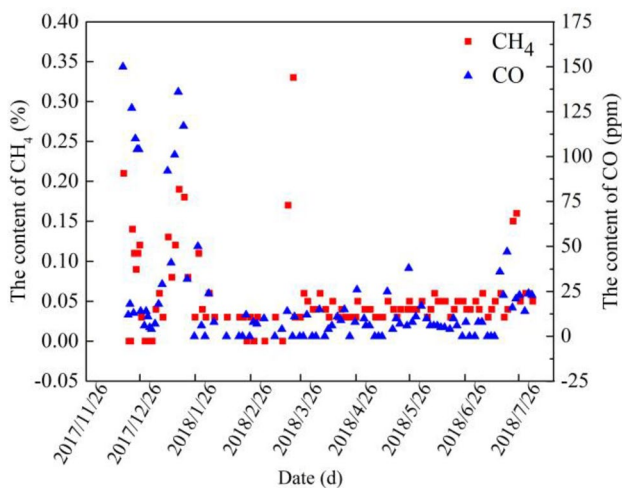


Fig. 16 The content of CH₄ and CO during tunnel construction

Organization of synchronous transportation in cable tunnel

Building material and trackless vehicle

Building materials utilized for the internal structural construction of cable tunnel are concrete segment, box culvert, concrete, cement mortar, slurry pipe, water pipe, and other auxiliary materials. If the transportation of building materials required for every 8 m is regarded as a synchronous transport cycle, 4 rings of tunnel linings with 32 concrete segments have to be assembled by segment erector. 6 precast box culverts need to be installed by crane. 2 slurry pipes and 4 water pipes are required for line extension. 96 m³ cement mortar is utilized for synchronous grouting. The requirements of concrete depend on the

Table 4 Building materials required for the internal structural construction of cable tunnel in a synchronous transport cycle

Materials	Requirements
Concrete segment	4 rings of tunnel linings (32 concrete segments) need to be assembled
Precast box culvert	6 box culverts need to be installed
Slurry/water pipe	2 slurry pipes and 4 water pipes need to be transported to the working face
Mortar	96 m ³ cement mortar needs to be transported to the working face
Concrete	45 m ³ /d concrete is required for the construction of side box culvert

construction progress of side box culvert. Statistics indicate that the average volume is 45 m³/day. Building materials required for the internal structural construction of cable tunnel in a synchronous transport cycle are illustrated in Table 4.

Trackless vehicles are utilized for the transportation of building materials. Their performance parameters are illustrated in Table 5. Taking the dual-headed truck G as an example, since 4 concrete segments are loaded at each time, 8 dual-headed trucks G (numbered from G₁ to G₈) are applied to transport 32 concrete segments in a synchronous transport cycle. A similar method has been used to estimate the number of dual-headed trucks X, D, and truck S. The results indicate that 3 dual-headed trucks X (numbered from X₁ to X₃), 1 dual-headed truck D (numbered D₁), and 24 trucks S (numbered from S₁ to S₂₄) are required for the transportation of 6 precast box culverts, 6 pipes (including 2 slurry pipes and 4 water pipes) and 96 m³ cement mortar. As for truck H, the number is stable at about 9 (numbered from H₁ to H₉) per day.

Vehicle scheduling model

As for Sutong GIL Yangtze River Crossing Cable Tunnel, four tunnel lining rings need to be assembled in a synchronous transport cycle. Taking the transportation of building materials for each tunnel lining ring as a single transportation cycle, there are four single transportation cycles numbered I, II, III, and IV in each synchronous transportation cycle. Trackless vehicles required for material transportation in each single transportation cycle are listed in Table 6.

Trackless vehicles in the single transportation cycle numbered IV are different from those in the single transportation cycles numbered I, II, and III. Instead of the dual-headed truck X, the dual-headed truck D is required for the transportation of slurry pipelines and water pipelines. Since the average speed is identical (Table 5), the driving time of the dual-headed trucks X from tunnel portal to working face should be identical with that of the dual-headed trucks D. As for unloading time, the dual-headed truck X is 0.33 h, while the dual-headed truck D is 0.17 h. So, the total time (including the driving time and unloading time) of the single transportation cycle numbered IV is less than that of the single transportation cycles numbered I, II, and III. If the single transportation cycle numbered I (or II, or III) is regarded as a standard single transportation cycle, the transportation of building materials in the single transportation cycle numbered IV can be completed on time.

Taking the standard single transportation cycle I as an example, 3 dual-headed trucks and 6 trucks are required for transportation and unloading. The initial state is considered to be that the dual-headed truck numbered X₁ and the truck numbered S₅ are unloading and the truck numbered S₆ is waiting for unloading at the parking platform. If a double-headed truck followed by two trucks is arranged for transporting and unloading each time, the standard single transportation cycle can be divided into six sections (numbered from Section 1 to 6). The vehicle scheduling model in the six sections is shown in Table 7 and Fig. 17.

Trucks H drive almost in the three-lane section where one vehicle can give another the right of way. Although they need to be parked on the single lane for unloading, the

Table 5 Performance parameters of trackless vehicles utilized for the transportation of building materials

Trackless vehicle	Transport capacity	Average speed of empty truck V _{i1} (km/h)	Average speed of full-loaded truck V _{i2} (km/h)	Unloading time T _{i3} (h)
Dual-headed truck G	4 concrete segments	5.7	9	0.33
Dual-headed truck X	2 box culverts	5.7	9	0.33
Dual-headed truck D	6 slurry/water pipes	5.7	9	0.17
Truck S	4 m ³ mortar	20	25	0.13
Truck H	5 m ³ concrete	20	25	0.33

The auxiliary materials such as pipe bracket and sealing grease are transported simultaneously by the double-headed trucks G, D, and X. The average speed and unloading time of trackless vehicles are obtained by field measurement

Table 6 Trackless vehicles required for material transportation in the single transportation cycle

Serial number	Trackless vehicle
I	Dual-headed trucks G ₁ , G ₂ , X ₁ ; Trucks S ₁ , S ₂ , S ₃ , S ₄ , S ₅ , S ₆
II	Dual-headed trucks G ₃ , G ₄ , X ₂ ; Trucks S ₇ , S ₈ , S ₉ , S ₁₀ , S ₁₁ , S ₁₂
III	Dual-headed trucks G ₅ , G ₆ , X ₃ ; Trucks S ₁₃ , S ₁₄ , S ₁₅ , S ₁₆ , S ₁₇ , S ₁₈
IV	Dual-headed trucks G ₇ , G ₈ , D ₁ ; Trucks S ₁₉ , S ₂₀ , S ₂₁ , S ₂₂ , S ₂₃ , S ₂₄

passage of other trackless vehicles will not be disturbed. Because the unloading of concrete is arranged to be synchronously with that of concrete segment and box culvert, there will be no vehicles driving through the concrete unloading section in this period. The concrete pouring is carried out three times a day. Since the concrete required for side box culvert is 10 m³, 10 m³, and 25 m³, the number of trucks H should be 2, 2, and 5 respectively.

With the application of vehicle scheduling model, the traffic congestion has been alleviated and the transportation efficiency has been improved. Compared with the original vehicle scheduling scheme, the number of required vehicles has decreased from 9 to 6. The retention time of vehicles at the waiting area has decreased from 166 to 35 min. The vehicle scheduling model has improved trackless vehicle transportation capacity and tunnel structure construction efficiency.

Environmental control equipment for dust-free installation

In order to ensure that the installation environment of 1000-kV GIL equipment satisfies the requirements, an environmental control equipment has been developed and applied at Sutong GIL Yangtze River Crossing Cable Tunnel. As shown in Fig. 18, it consists of transparent PVC (polyvinyl chloride) cloth, front scaffold, rear scaffold, beam component, and mobile air shower. The transparent PVC cloth is attached to the outside of the environmental control equipment. It not only ensures the air tightness of the environmental control equipment, but also allows the visualization of the GIL equipment installation. The front scaffold is configured with electric devices such as dehumidification equipment and lighting lamp. The rear scaffold is not only the critical component of the structural support, but also the installation platform of the air filter equipment. Two air filter equipment

are installed on both sides of the rear scaffold respectively. After two-stage filtration of the high-efficiency particulate air (HEPA) composite glass fiber filter (the filtration accuracy is up to 0.3 μm), the clean air is blown into the environmental control equipment. The dusty gas in the environmental control equipment can be discharged by the Velcro joints on the transparent PVC cloth. As the air circulates, the dusty gas in the environmental control equipment will be purified. The GIL equipment can only be installed when the air cleanliness satisfies ISO Class 9 (ISO E. 14644–1 1999).

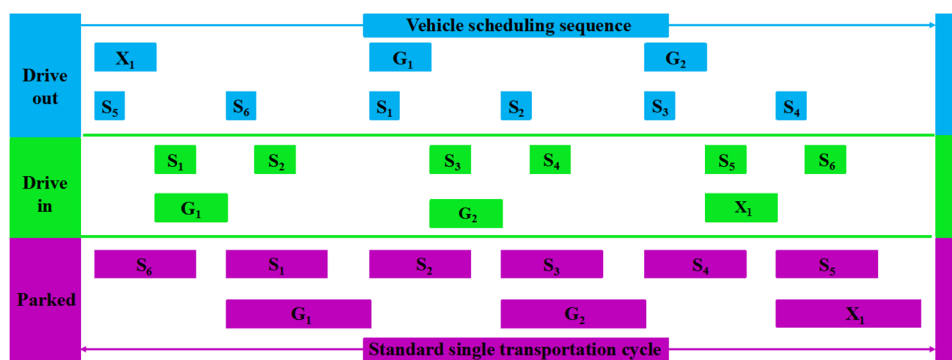
The construction of the environmental control equipment in the limited tunnel interior space is difficult. Before scaffold installation, high-precision tracks should be laid along the tunnel alignment. The orbital error and elevation error should not exceed 4 mm (chord length 10 m), while the gauge error and horizontal error should not exceed −2~+3 mm and 4 mm (GB 10183–2010 2010; TB 10082–2017 2017). Then, the front scaffold and rear scaffold should be moved from the previous working surface to the current working surface along the middle track and the side track respectively. Next, the front scaffold, rear scaffold, and connecting components should be spliced to complete the structure of environmental control equipment. Finally, the transparent PVC cloth should be attached to the outside of the environmental control equipment for air tightness.

With the application of newly developed environmental control equipment, the air cleanliness around GIL equipment has reached ISO Class 9 (ISO E. 14644–1 1999). The air humidity has been 56% (lower than 80%) and the illuminance has been 124 Lx (higher than 75 Lx), which has satisfied the Power Industry Standards of the People’s Republic of China (DL/T 5838–2021 2021). Under the protection of environmental control equipment, the GIL equipment with a length of more than 5400 m has been installed in 5 months without contamination.

Table 7 The vehicle scheduling model in six sections numbered from 1 to 6

Vehicles	Initial state	Section 1	Section 2	Section 3	Section 4	Section 5	Section 6
Drive out	-	X ₁ , S ₅	S ₆	G ₁ , S ₁	S ₂	G ₂ , S ₃	S ₄
Drive in	-	G ₁ , S ₁	S ₂	G ₂ , S ₃	S ₄	X ₁ , S ₅	S ₆
Parked	X ₁ , S ₅ , S ₆	S ₆ , G ₁ , S ₁	G ₁ , S ₁ , S ₂	G ₂ , S ₂ , S ₃	G ₂ , S ₃ , S ₄	X ₁ , S ₄ , S ₅	X ₁ , S ₅ , S ₆

Fig. 17 Vehicle scheduling model in the standard single transport cycle I (the length of the box is positively correlated with time)



Robot intelligent inspection of UHV cable tunnel

The framework of robot intelligent inspection system

In order to overcome the shortcomings of manual inspection in time-consuming, laborious, and inefficient, robot intelligent inspection system composed of inspection robot, carrier track, power supply, communication system, and management platform has been proposed for the inspection of cable tunnel (Fig. 19). The inspection robot is equipped with high-definition cameras, infrared cameras, partial discharge detectors, and environmental monitoring detectors. It allows real-time monitoring and diagnosis of cable tunnel and GIL equipment. The operation parameters and mobile video are transmitted by the communication system to the management platform for practical task management and personalized data presentation. With the real-time monitoring of equipment status and performance parameters, mechanical failure and hidden defect can be found in time, which facilitates the safe and efficient operation of the ultra-high-voltage cross-river cable tunnel.

The monitor items of intelligent inspection robot

As shown in Fig. 20, the inspection robot is composed of sliding mechanism, lifting mechanism, lifting warehouse, control warehouse, and terminal platform. The sliding mechanism allows inspection robot moving along alloy track. The lifting warehouse and lifting mechanism are retractable, which allows inspection robot to monitor the operation status of cable equipment with different elevations. The control warehouse is equipped with temperature sensor, humidity sensor, gas sensor, and smoke sensor, while the terminal platform is furnished with thermal imaging camera, high-definition camera, partial discharge detector, and ultrasonic flaw detector. With the complete monitoring system installed on the inspection robot, the following items can be monitored in real time:

1. Structural damage monitoring: the high-definition video and preset point calibration enable lining deformation monitoring and structural joint dislocation, while the image recognition and comparison allow precise localization and corrosion identification of casing equipment and fastening components.

Fig. 18 The environmental control equipment for the installation of 1000 kV GIL equipment

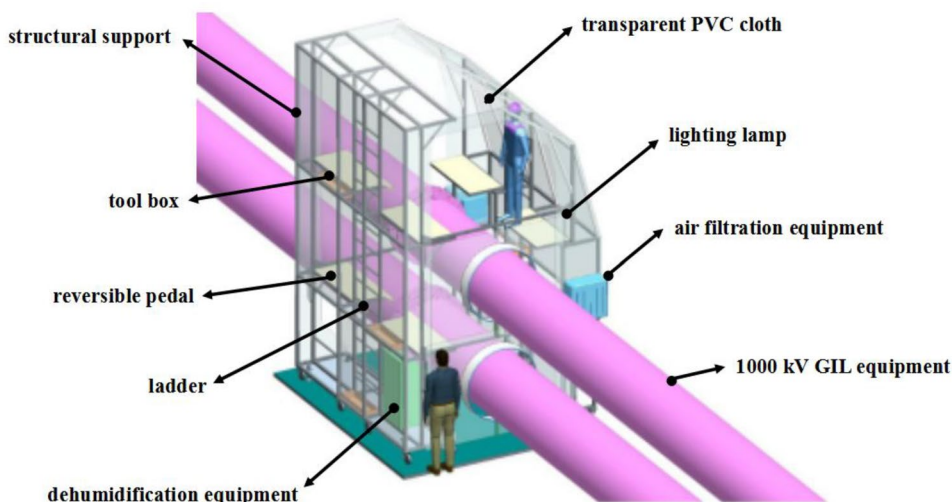
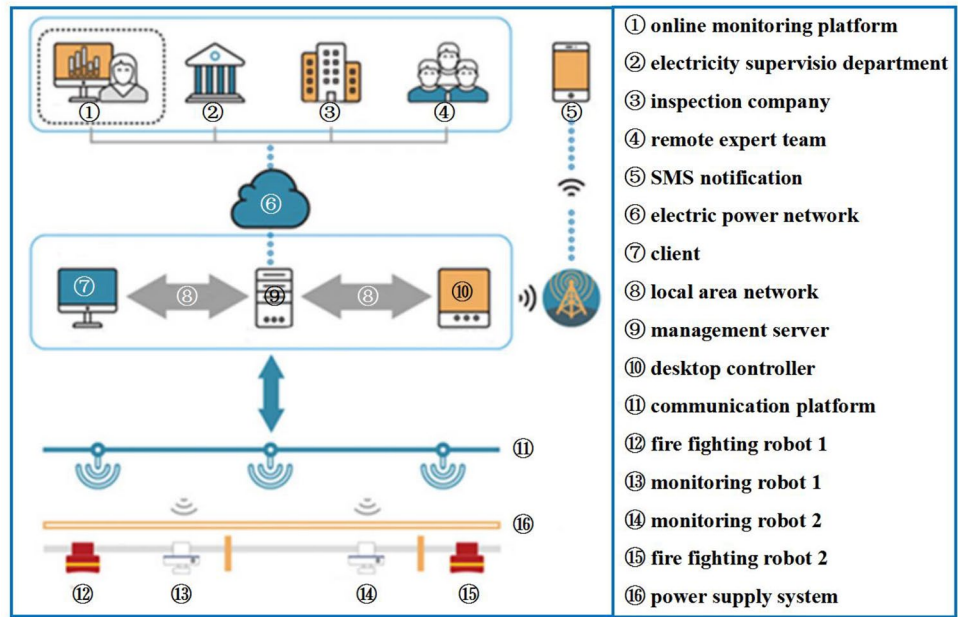


Fig. 19 The framework of robot intelligent inspection system



2. Infrared temperature monitoring: the infrared imaging technology allows the inspection robot to measure the surface temperature of cable equipment and surrounding environment when sliding along the alloy track.
3. Gas parameter monitoring: the gas monitoring module allows monitoring the content of O₂, H₂S, CO, CH₄, SF₆ (The SF₆ is filled in the GIL equipment as an insulating medium. Once gas leakage occurs, it will penetrate into the tunnel.), humidity, and smoke in the cable tunnel.
4. Partial discharge monitoring: partial discharges of electrical equipment may occur under high-voltage or elec-

tromagnetic environment. The partial discharge sensor detects cable equipment defects and prevents power transmission failures.

The operation mode of intelligent inspection robot

The operation mode of the intelligent inspection robot can be divided into four categories. They are automatic inspection, remote inspection, special inspection, and cooperative inspection. Details are as follows:

1. Automatic inspection mode: It is the most common inspection mode in the daily operation of cable tunnel. The robot inspects the working condition of electric equipment along the preset route. The visual inspection, temperature diagnosis, and gas detection of equipment in the comprehensive warehouse and power warehouse will be carried out continuously. Equipment status and performance parameters will be transmitted to the integrated management platform.
2. Remote inspection mode: it is suitable when the robot detects the abnormal equipment status or performance parameters. In accordance with remote control commands, the lifting mechanism will move along the rod to adjust the elevation of cameras and detectors. The terminal platform will rotate to adapt the camera lens multiples to obtain high-definition images of equipment and environment.
3. Special inspection mode: as a supplement to automatic inspection mode and remote inspection mode, it is formulated for special inspection of key objects (such as 1000 kV GIL equipment, 500 kV cable) in the cable tunnel.

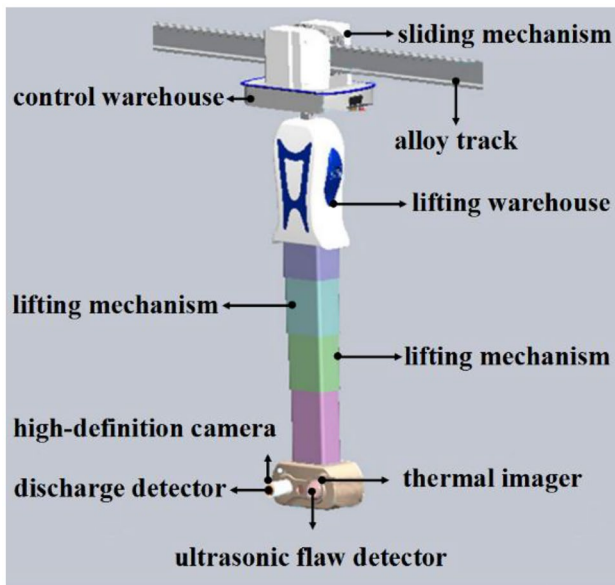
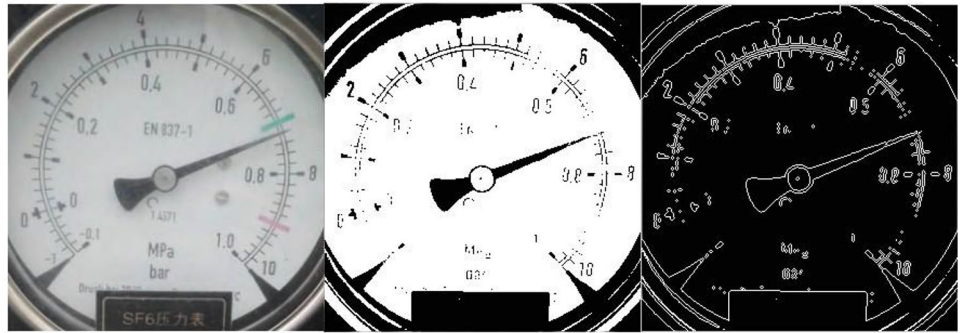


Fig. 20 Schematic diagram of the inspection robot structure

Fig. 21 The processing of instrument pointer image



4. Cooperative inspection mode: It allows several robots to be installed on one track, and each robot is responsible for a specific inspection section. Once a robot is abnormal, the nearest robot will inspect this section on its behalf.

Four inspection modes cooperate with each other to allow the digital operation of long-distance cable tunnel. Once safety emergencies such as gas leakage, equipment short-circuit, and excessive temperature are monitored, manual intervention will be conducted in time to repair the damaged tunnel environment or electrical equipment.

Robot intelligent inspections have been conducted for tunnel internal environment and equipment operating condition. The tunnel structure, infrared temperature, gas parameter, and partial discharge have been monitored in real time. Taking video monitoring of instrument readings as an example, it is necessary to convert the captured image into the grayscale image to eliminate the influence of background (Fig. 21). The instrument pointer can be separated from the instrument panel by binary processing. The binary processing image has illustrated a straight line feature to facilitate pointer recognition. Then, the image information has been transformed by Hough transform to obtain the angle of the thinning pointer line. The meter reading can be obtained according to pointer angle. It has been transmitted to the control system for warning identification. With the application of robot intelligent inspections, tunnel environment has been well maintained and GIL equipment has been efficiently operated for more than 2 years.

Conclusions

The present study focused on the construction and inspection of the first underwater gas-insulated transmission line for 1000 kV power in the world, Sutong GIL Yangtze River Crossing Cable Tunnel. Engineering features and construction challenges have been analyzed. Key technologies have been developed and applied for safety and efficient

construction and inspection of long-distance cross-river cable tunnel. From the present study, the following conclusions can be made:

1. In order to minimize the Yangtze River embankment deformation, tunneling parameters including slurry pressure, grouting material, and grouting pressure have been improved. Embankment deformation has been monitored to ensure that the maximum value has been lower than the limited value.
2. Construction technologies have been proposed for biogenetic gas ground tunneling. The clay shock method has prevented biogenetic gas from seeping into tunnel. Methane detector system and explosion-proof design have minimized the risk of gas explosion. Gas extraction system has exhausted biogenetic gas in tunnel.
3. In order to minimize the risk of traffic congestion in the single lane, the vehicle scheduling model has been proposed for the organization of material transportation. The application of vehicle scheduling model during the tunnel construction has satisfied the transportation requirements for building material well.
4. Environmental control equipment has been developed for the installation of 1000 kV ultra-high-voltage GIL equipment. With the environmental control equipment, air cleanliness has satisfied the ISO Class 9, air humidity has been 56% (lower than 80%), and the illuminance has been 124 Lx (higher than 75 Lx).
5. Intelligent inspection system has been proposed for the inspection of cable tunnel. With the complete monitoring system and inspection mode, tunnel environment and electrical equipment have been monitored automatically and cable tunnel can be operated digitally.

Funding Financially supported by the fellowship of China Postdoctoral Science Foundation (Grant No. 2022TQ0241), Key Research and Development Program of Hubei Province (Grant No. 2021BCA154), and State Grid Jiangsu Electric Power Co., Ltd. Economic Research Institute (Grant No. JSJS1600328) is gratefully acknowledged.

Declarations

Conflict of interest The authors declare no competing interests.

References

- Abdullah RA (2016) A review on selection of tunneling method and parameters effecting ground settlements. *Mal Eng* 21
- Alavi Gharahbagh E, Qiu T, Rostami J (2013) Evaluation of granular soil abrasivity for wear on cutting tools in excavation and tunneling equipment. *J Geotechn Geoenviron Eng* 139(10):1718–1726
- Agnisarman S, Lopes S, Madathil KC, Piratla K, Gramopadhye A (2019) A survey of automation-enabled human-in-the-loop systems for infrastructure visual inspection. *Autom Constr* 97:52–76
- Aydan Ö, Hassanpour R (2019) Estimation of ground pressures on a shielded TBM in tunneling through squeezing ground and its possibility of jamming. *Bull Eng Geol Environ* 78(7):5237–5251
- Benato R, Paolucci A (2010) *EHV AC undergrounding electrical power. Performance and Planning*, Springer, London (Series:Power Systems, ISBN: 978–1–84882–866–7)
- Bian ZD (2015) Clay shock and its construction method for shield machine. Chinese patent CN104291775A[P] 2015–01–21 (in Chinese)
- Bilgin N, Acun S (2021) The effect of rock weathering and transition zones on the performance of an EPB-TBM in complex geology near Istanbul. *Turkey Bull Eng Geol Environ* 80(4):3041–3052
- Bouayad D, Emeriault F (2017) Modeling the relationship between ground surface settlements induced by shield tunneling and the operational and geological parameters based on the hybrid PCA/ANFIS method. *Tunn Undergr Space Technol* 68:142–152
- Canto-Perello J, Curiel-Esparza J, Calvo V (2016) Strategic decision support system for utility tunnel’s planning applying A’WOT method. *Tunn Undergr Space Technol* 55:146–152
- Chen P, Wu J, Zhang XP, Xie WQ, Sun MZ, Tu XB (2018) Research on optimization model of trackless transportation in long-distance and large-diameter slurry shield tunnel: a case study of Sutong GIL utility tunnel. *Tunn Constr* 38(6):1022–1028 (in Chinese)
- Dai ZY, Yi JJ, Zhang YJ, Zhou B, He L (2020) Fast and accurate cable detection using CNN. *Appl Intel* 50(12):4688–4707
- Delmastro C, Lavagno E, Schranz L (2016a) Energy and underground. *Tunn Undergr Space Technol* 55:96–102
- Delmastro C, Lavagno E, Schranz L (2016b) Underground urbanism: master plans and sectorial plans. *Tunn Undergr Space Technol* 55:103–111
- Du GT, Cheng YF (2017) Application of clay shock injection technique in shield tunneling through major risk sources. *High Traffic Technol (applied Technology Edition)* 13(3):190–192 (in Chinese)
- Ding WQ, Duan C, Zhu YH, Zhao TC, Huang DZ, Li PN (2019) The behavior of synchronous grouting in a quasi-rectangular shield tunnel based on a large visualized model test. *Tunn Undergr Space Technol* 83:409–424
- Fang YS, Wu CT, Chen SF, Liu C (2014) An estimation of subsurface settlement due to shield tunneling. *Tunn Undergr Space Technol* 44:121–129
- Feng K, Cheng TJ, Dai ZC, He C, Wang SQ, Zhang ZB (2016) Safety assessment 440 of trackless transportation system in shield tunnels based on fuzzy comprehensive 441 evaluation. *Mod Tunnel Technol* 53(5):137–144 (in Chinese)
- Goel RK, Jethwa JL, Paithakan AG (1995) Tunneling through the young Himalayas—a case history of the Maneri-Uttarakashi power tunnel. *Eng Geol* 39:31–44
- Gui MW, Chen SL (2013) Estimation of transverse ground surface settlement induced by DOT shield tunneling. *Tunn Undergr Space Technol* 33:119–130
- Guo F, Gao F, Ma HG, Guo S (2013a) Study on trackless tyred vehicle intelligent scheduling system base on time response. *Appl Mech Mater* 373:1525–1528
- Guo F, Gao F, Guo S, Ma HG (2013b) Research on the transport line of the trackless rubber tire vehicle underground coal mine. *Appl Mech Mater* 373:2284–2287
- Guo XJ, Dai HW (2013) Study and application of river-crossing technology for super-large slurry shield: Nanjing Yangtze River-crossing Tunnel. China Architecture and Building Press, Beijing (In Chinese)
- Hashemnejad A, Hassanpour J (2017) Proposed soil classification based on the experiences of soft-ground tunneling in Iran. *Bull Eng Geol Environ* 76(2):731–750
- He Z (2016) Study on program optimization of cable tunnel constructions on GR-T fuzzy number multi-attribute decision making (Master’s thesis, Shijiazhuang Tiedao University) (In Chinese)
- Home L (2010) Trends in the use of TBMs worldwide. Presented at NFF TBM seminar Bergen
- Hong QY, Lai HP, Liu YY, Ma XM, Xie JT (2021) Deformation control method of a large cross-section tunnel overlaid by a soft-plastic loess layer: a case study. *Bull Eng Geol Environ* 80(6):4717–4730
- ISO E. 14644–1 (1999) “Cleanrooms and associated controlled environments—part 1: classification of air cleanliness”. European Standard
- Jia Y, Yang LC, Liu JG (2012) Transportation matching design of earth pressure balance shield in medium distance tunnel. *Adv Mater Res* 368:2526–2532
- Jakobsen PD, Lohne J (2013) Challenges of methods and approaches for estimating soil abrasivity in soft ground TBM tunnelling. *J Wear* 308(1–2):166–173
- Jiménez VJH, Castronuovo ED, Sánchez I (2018) Optimal statistical calculation of power cables disposition in tunnels, for reducing magnetic fields and costs. *Int J Electr Power Energy Syst* 103:360–368
- Jin DL, Yuan DJ, Li XG, Zheng HT (2018) Analysis of the settlement of an existing tunnel induced by shield tunneling underneath. *Tunn Undergr Space Technol* 81:209–220
- Kaliampakos D, Benardos A, Mavrikos A, Panagiotopoulos G (2016) The underground atlas project. *Tunn Undergr Space Technol* 55:229–235
- Kasper T, Meschke G (2006) On the influence of face pressure, grouting pressure and TBM design in soft ground tunnelling. *Tunn Undergr Space Technol* 21(2):160–171
- Li HQ, Fan YQ, Yu MJ (2018) Deep Shanghai project—A strategy of infrastructure integration for megacities. *Tunn Undergr Space Technol* 81:547–567
- Li XC, Li XG, Yuan DJ (2017) Application of an interval wear analysis method to cutting tools used in tunneling shields in soft ground. *J Wear* 392:21–28
- Li YZ, Ingason H (2018) Overview of research on fire safety in underground road and railway tunnels. *Tunn Undergr Space Technol* 81:568–589
- Liang JH, Zhang XP, Xie WQ, Wu J, Chen P, Sun MZ, Qian YH, Huang YT (2018) Research on vehicles scheduling model in single lane of long-distance and large-diameter shield tunnel. *Tunn Constr* 38(S2):218–226 (in Chinese)
- Lin CG, Zhang ZM, Wu SM, Yu F (2013) Key techniques and important issues for slurry shield under-passing embankments: a case study of Hangzhou Qiantang River Tunnel. *Tunn Undergr Space Technol* 38:306–325
- Magier T, Tenzer M, Koch H (2017) Direct current gas-insulated transmission lines. *IEEE Trans Power Delivery* 33(1):440–446
- Masuda T, Yumura H, Watanabe M (2008) Recent progress of HTS cable project. *Physica C* 468(15–20):2014–2017
- Min FL, Zhu W, Lin C, Guo XJ (2015) Opening the excavation chamber of the large-diameter size slurry shield: a case study

- in Nanjing Yangtze River Tunnel in China. *Tunn Undergr Space Technol* 46:18–27
- Moghaddasi MR, Noorian-Bidgoli M (2018) ICA-ANN, ANN and multiple regression models for prediction of surface settlement caused by tunneling. *Tunn Undergr Space Technol* 79:197–209
- Montero R, Victores JG, Martínez S, Jardón A, Balaguer C (2015) Past, present and future of robotic tunnel inspection. *Autom Constr* 59:99–112
- Muir Wood AM (1994) The Thames Tunnel 1825–43: where shield tunnelling began. *Proc Inst Civi Eng: Civ Eng* 102(3)
- National Energy Administration (2021) DL/T 5838–2021 specification for construction quality checkout and evaluation of gas-insulated metal-enclosed 1000 kV transmission line in tubular tunnel. China Electric Power Press Beijing (in Chinese)
- National Mine Safety Administration of China (2004) Coal mine safety regulations. China Coal Industry Publishing House Press Beijing (in Chinese)
- National Railway Administration of the People's Republic of China (2017) TB 10082–2017 code for design of railway track. China Railway Press Beijing (in Chinese)
- Neumann C, Jürgens I, Alter J, Poehler S (2010) Pilot installation of a 380 kV directly buried gas insulated line (GIL). Set of Papers CIGRE Session
- Poehler S, Rudenko P (2012) Directly buried gas-insulated transmission lines (GIL). In PES T&D 2012 (pp. 1–5). IEEE
- Seet G, Yeo SH, Law WC, Wong CY, Sapari S, Liau KK (2018) Design of tunnel inspection robot for large diameter sewers. *Procedia Comput Sci* 133:984–990
- State Administration for Market Regulation (2010) GB 10183–2010 Grans-tolerances for wheels and travel and traversing tracks. China Standard Press Beijing (in Chinese)
- Tang SH, Zhang XP, Liu QS, Chen P, Sun XT, Sun L, Dai Y, Chen ST (2020) Prediction and analysis of replaceable scraper wear of slurry shield TBM in dense sandy ground: A case study of Sutong GIL Yangtze River Crossing Cable Tunnel. *Tunn Undergr Space Technol* 95:103090
- Tang SH, Zhang XP, Liu QS, Xie WQ, Yang XM, Chen P, Tu XB (2021a) Analysis on the excavation management system of slurry shield TBM in permeable sandy ground. *Tunn Undergr Space Technol* 113:103935
- Tang SH, Zhang XP, Liu QS, Xie WQ, Wu XL, Chen P, Qian YH (2021b) Control and prevention of gas explosion in soft ground tunneling using slurry shield TBM. *Tunn Undergr Space Technol* 113:103963
- Tang SH, Zhang XP, Liu QS, Xie WQ, Wang HJ, Li XF, Zhang XY (2022) New soil abrasion testing method for evaluating the influence of geological parameters of abrasive sandy ground on scraper wear in TBM tunneling. *Tunn Undergr Space Technol* 128:104604
- Tenzen M, Koch H, Imamovic D (2016) Underground transmission lines for high power AC and DC transmission. In 2016 IEEE/PES Transmission and Distribution Conference and Exposition (T&D) (pp. 1–4). IEEE
- Tobriner S (1984) A history of reinforced masonry construction designed to resist earthquakes: 1755–1907. *Earthq Spectra* 1(1):125–149
- Vähäaho I (2016) An introduction to the development for urban underground space in Helsinki. *Tunn Undergr Space Technol* 55:324–328
- Victores JG, Martínez S, Jardón A, Balaguer C (2011) Robot-aided tunnel inspection and maintenance system by vision and proximity sensor integration. *Autom Constr* 20(5):629–636
- Wang XH, Song YH, Jung CK, Lee JB (2007) Tackling sheath problems: latest research developments in solving operational sheath problems in underground power transmission cables. *Electr Power Syst* 77(10):1449–1457
- Wang JJ, Yuan WH, Liu Y, Guo J (2016a) Development present situation and the analysis of common disasters of existing electric power tunnel in Beijing. *Constr Qual* 34(11):75–78 (In Chinese)
- Wang Q, Wang SY, Sloan SW, Sheng DC, Pakzad R (2016b) Experimental investigation of pressure grouting in sand. *Soils Found* 56(2):161–173
- Wang TY, Tan LX, Xie SY, Ma BS (2018) Development and applications of common utility tunnels in China. *Tunn Undergr Space Technol* 76:92–106
- Xie XY, Yang YB (2012) A method for dynamic risk assessment of the operating power tunnel. *GeoCongress 2012: State of the art and practice in geotechnical engineering* pp 4339–4347
- Xu F, Wang L, Wang XS, Jiang GP (2013) Dynamic performance of a cable with an inspection robot—analysis, simulation, and experiments. *J Mech Sci Technology* 27(5):1479–1492
- Yang C, Peng FL (2016) Discussion on the development of underground utility tunnels in China. *Proc Eng* 165:540–548
- Yang SQ (2016) Study on key technologies of urban transmission tunnel construction. (Master's thesis, Zhengzhou University) (In Chinese)
- Yang TH, Zheng QH, Wang Y, Wang SF (2013) Safety risk analysis of underground power cable infrastructure in a city. In ICPTT 2012: Better Pipeline Infrastructure for a Better Life pp 1459–1470
- Yao QY, Di HG, Ji C, Zhou SH (2020) Ground collapse caused by shield tunneling in sandy cobble stratum and its control measures. *Bull Eng Geol Environ* 79(10):5599–5614
- Yu B, Wu SH, Yao BZ, Yang ZZ, Sun J (2012) Dynamic vehicle dispatching at a transfer station in public transportation system. *J Transp Eng* 138(2):191–201
- Zhang CP, Zhang X, Fang Q (2018a) Behaviors of existing twin subway tunnels due to new subway station excavation below in close vicinity. *Tunn Undergr Space Technol* 81:121–128
- Zhang DM, Huang ZK, Wang RL, Yan JY, Zhang J (2018b) Grouting-based treatment of tunnel settlement: practice in Shanghai. *Tunn Undergr Space Technol* 80:181–196
- Zhang DM, Huang ZK, Yin ZY, Ran LZ, Huang HW (2017) Predicting the grouting effect on leakage-induced tunnels and ground response in saturated soils. *Tunn Undergr Space Technol* 65:76–90
- Zhang XP, Tang SH, Liu QS, Tu XB, Chen P, Li FY (2021) An experimental study on cutting tool hardness optimization for shield TBMs during dense fine silty sand ground tunneling. *Bull Eng Geol Environ* 80(9):6813–6826
- Zhao Y, Li G, Liu Q, Tan J (2017) Study on operation and structural disaster of power tunnel in Beijing. *Electrotech Appl* 7:28–32 (In Chinese)
- Zhao YC, Zhu GQ, Gao YJ (2018) Experimental study on smoke temperature distribution under different power conditions in utility tunnel. *Case Stud Therm Eng* 12:69–76

Springer Nature or its licensor (e.g. a society or other partner) holds exclusive rights to this article under a publishing agreement with the author(s) or other rightsholder(s); author self-archiving of the accepted manuscript version of this article is solely governed by the terms of such publishing agreement and applicable law.